BOLETIN DE LA SOCIEDAD ESPAÑOLA DE
Cerámica y Vidrio
ARTICULO

Chemical interaction silicon nitride ceramics and iron alloys

F.J. OLIVEIRA, R.F. SILVA, J.M. VIEIRA
Department of Ceramics and Glass Engineering, UIMC, University of Aveiro, 3810-193 Aveiro, Portugal

Metal/ceramic diffusion experiments are helpful to study bonding mechanisms or the effect of metal composition on the chemical wear of ceramic cutting tools. The reaction kinetics of Fe alloys/Si_3N_4 ceramic diffusion couples was investigated in the temperature range 1050ºC-1250ºC, for 0.5h to 80h, under inert atmosphere. Optical microscopy, SEM and EPMA were carried out in cross sections of the reacted pairs. Si_3N_4 decomposes into Si and N that dissolve and diffuse through the metal. Both the diffusion zone on the metal side and the reaction zone on the ceramic side obey parabolic growth laws of time, with activation energies in the range Q=310-460kJmol^{-1}. The amount of dissolved Si, the length of the diffusion zone and thus the reactivity of the ceramic increase as the alloy carbon content decreases. Due to Si accumulation, the α-Fe solid solution is stabilised at the reaction temperature and a steep decrease in the Si concentration is observed beyond the diffusion zone. The reinforcement of the Si_3N_4 composites with $A1_2O_3$ platelets enhances the chemical resistance of the ceramic due to the inertness of this oxide and to the partial crystallisation of the intergranular phase. Other dispersoids such as HfN, BN and TiN do not improve the chemical resistance of the matrix by iron attack.

Keywords: silicon nitride, steels, diffusion couples, interface kinetics

Interacción químico entre nitruros de silicio y aleaciones de acero

Los experimentos de difusión metal/cerámica permiten estudiar mecanismos de unión y analizar el efecto de la composición del metal en el desgaste químico de herramientas de corte cerámicas. En este trabajo se investigó la cinética de reacción en pares de difusión aleaciones de Fe/Si_3N_4 a temperaturas entre 1050ºC-1250ºC, tiempos entre 0.5h a 80h, en atmósfera inerte. Las secciones transversales de los pares de difusión se analizaron mediante microscopía óptica, SEM y microsonda electrónica. El Si_3N_4 se descompone en Si y N que se disuelven y difunden en el metal. Tanto la zona de difusión en el metal como la zona de reacción en la cerámica obedecen una ley parabólica de crecimiento, con energías de activación de 310-460 KJ.mol-1. La cantidad de Si disuelto, el tamaño de la zona de difusión y, por lo tanto, la reactividad de la cerámica aumenta al diminuir el contenido de carbón de la aleación. Debido a la acumulación de Si, la solución sólida de a-Fe se estabiliza a la temperatura de reacción, y se observa un descenso significativo en la concentración de Si más allá de la zona de difusión. El reforzamiento del Si_3N_4 con plaquetas de Al_2O_3 aumenta la resistencia química del Si_3N_4 debido a la inercia de este oxido y a la cristalización parcial de la fase intergranular. La incorporación de HfN, BN y TiN no mejoran la resistencia química de la matriz al ataque por Fe.

Palabras clave: nitruro de silicio, aceros, pares de difusión, cinética de interfases

1. INTRODUCTION

Silicon nitride (Si_3N_4) ceramics are currently being used as wear parts and engine components. For a successful use in applications that may have intricate geometry, bonding to a different material or to itself is often a requirement [1,2]. Brazing can be done at temperatures below 900ºC, thus limiting the maximum useful temperature of the component [3]. Direct bonding to refractory metals or alloys of higher melting points, such as Fe or Ni base alloys are alternative methods still under study [4]. The interactions between iron alloys and Si_3N_4 ceramics are of importance also in the field of cutting tools [5-7]. It is well known that silicon nitride cutting tools wear rapidly in high speed machining of most steels, while being able of machining grey cast iron with minimum wear rates [8]. Kramer and Suh [9] have proposed a model where the solubility of the tool material in pure iron determines the wear rate relative to HfC. Vleugels et al. [10] developed Kramer´s model to account for the effect of the iron alloy composition on the wear rate of silicon nitride cutting tools. In this model, the chemical affinity between alloying elements and the nitrogen determines the reactivity of a given alloy. Silva and others [7] further improved the theoretical approach, considering the chemical cross effects of alloying elements on both Si and N originating from ceramic decomposition.

These approaches are established on a thermodynamic basis and further improvements are needed concerning the reaction kinetics. Solid state diffusion couples have been used as way of determining the reaction rates of Si_3N_4 or SiAlON ceramics in contact with Fe alloys [2,10]. The study of interactions between the Si_3N_4 ceramics and the iron alloys should bring about the effects of alloys compositions and ceramic sintering additives on the reaction mechanisms. The incorporation of nitride and oxide compounds of large negative Gibbs energy of formation also affects the overall chemical resistance of the Si_3N_4 ceramics in the contact with iron alloys [11]. In the present work, the reactivity of several Si_3N_4 monolithic and composite ceramic materials in diffusion couples with pure Fe, carbon and chromium alloyed steels is investigated. Equilibrium thermodynamic calculations at moving interphase boundaries in the metal are tentatively correlated to concentration profiles of Si diffusing from the ceramic side of the couple.

2. EXPERIMENTAL DETAILS

Metal/ceramic diffusion couples, produced under inert atmosphere or vacuum, were used to study the reaction kinetics at temperatures in the range 1050ºC-1250ºC for dwelling times of 0.5h to 80h. The experimental set up and the geometry of the diffusion couples have been described in previous publications [12,13,14]. A thin piece of ceramic (60-150μm) is placed between two larger steel slabs that forge around the ceramic at the reaction temperature. Alumina platelets (Grade T2, ELF ATOCHEM) were placed between the ceramic and the steel to mark the initial contact plane. The couples are supported with alumina spacers in a graphite jig, inside an alumina tube with water cooled caps. The load is applied using a cantilever to values between 5MPa and 7.5MPa.

Several silicon nitride (Si_3N_4) based ceramics were developed (Table I) to study the effect of matrix composition and of reinforcing phases on the reactivity in contact with iron alloys. The hardness of the ceramics was measured using Vickers indentation at 10kg load and K_{1c} was calculated from the length of the indentation cracks, using the well-known Anstis equation:

$$K_{1c} = 0{,}016\left(\frac{E}{H_v}\right)^{1/2}\frac{P_D}{c_f^{3/2}} \quad [15].$$

The Si_3N_4 monolithic material (SN1) was fully densified by hot-pressing at 1650ºC/30MPa/60min. A somewhat higher temperature (1700ºC/120min/30MPa) was necessary for densification of the composites with the SN1 matrix to overcome the constraining effects of the inclusions upon sintering. The composite containing the alumina platelets (SN2-AL) was developed aiming a reduction of dissolution of the reinforcing phase, by saturating with Al_2O_3 the intergranular glassy phase always present in silicon nitride ceramics [16]. This composite was hot-pressed at 1500ºC/90min/30MPa. All the ceramics were hot-pressed in a BN coated graphite die, thermally insulated with coarse alumina powder, and heated in air by a radio frequency induction generator.

The study of the effect of iron alloys composition on the reaction kinetics was done with pure iron and five commercially available steels with different amounts of carbon and chromium (Table II). The iron alloys are three carbon steels with increasing amount of carbon, A1, A2 and A3 and two chromium containing steels, AC1 and AC2 where AC1 has less carbon than AC2.

After reaction, the metal/ceramic interface was cross-sectioned and polished for observation and chemical analysis by scanning electron microscopy (SEM- Hitachi S4100) and electron probe microanalysis (EPMA -Cameca). Calibration of the EPMA with Cr, Fe and Si standards was made prior to the analyses while the SEM/EDS system used software calibration methods. Although detectable, carbon and nitrogen were not quantified in either of these two systems, due to contamination in the case of carbon, and due to the low amount of nitrogen that was below the detection limit of the EPMA (about 0.04wt%). The length of the affected zones on both the ceramic and the iron alloys was evaluated using an optical microscope (Zeiss) and the image analysis software Quantimet 500+ (Leica Cambridge).

TABLE I. COMPOSITION AND MECHANICAL PROPERTIES OF THE CERAMIC MATERIALS USED IN THE DIFFUSION EXPERIMENTS.

Code	Matrix Composition				Reinforcement (30vol%)	H_V (GPa)	K_{1c} (MPam$^{1/2}$)
	[1] Si_3N_4 (wt%)	[2] CeO_2 (wt%)	[3] AlN (wt%)	[4] Al_2O_3 (wt%)			
SN1	89.0	5.0	6.0	-	-	17.2	3.4
SN1-BN	"	"	"	-	BN (Grade A01, H.C. Starck)	4.5	3.7
SN1-HN	"	"	"	-	HfN (Johnsson Matthey)	15.6	6.2
SN1-TN	"	"	"	-	TiN (Submicron, Ceramyg)	14.6	5.8
SN2-AL	87.5	-	-	12.5	Al_2O_3 (Grade T2 Platelets, Elf Atochem)	19.1	4.6

[1] M11, H. C. Starck; [2] Fluka puriss.; [3] Grade C, H. C. Starck; [4] Al16SG, Alcoa

TABLE II. COMPOSITION OF THE IRON ALLOYS TESTED IN THE DIFFUSION COUPLES.

		Composition (wt%)				
Code	DIN	C	Cr	Mn	Si	others
[a] Fe	-	-	-	-	-	
A1	St 37 K	0.13	-	0.60	0.28	0.027S
A2	CK 45	0.473	-	0.61	0.24	0.009S; 0.02P
A3	C 105 W 1	1.05	-	<0.25	<0.25	
AC1	x 20 Cr 13	0.21	13.0	<1.0	<1.0	
AC2	x 210 Cr 13	2.07	11.41	0.32	0.39	0.001S; 0.015P

[a] Fe: Aldrich, 99,98% purity (65ppm Na, 60ppm Si, 25ppm Al, 5ppm Ti, 3ppm Ca, 1ppm Mg)

3. RESULTS AND DISCUSSION

Silicon nitride decomposes in contact with the iron alloys for all the experimental conditions tested in this work, the Si and N diffusing into the metal, leading to a diffusion zone of variable thickness, *d*, on the metal side of the couples (Figure 1a). EPMA analyses evidenced that Si remains in the metal adjacent to the ceramic while no N was detected. The low nitrogen partial pressures in the reaction chamber (0,5Pa for the Ar N50, Ar Líquido) and the low solubility of nitrogen in Fe at these temperatures [17] give rise to an easy escape of N to the atmosphere. The effect of nitrogen partial pressure on the reactivity was already assessed by others [18,19], the reactivity being highest for the lowest nitrogen partial pressure.

The additives of SN1 remain as oxides or mixed oxides in a zone of thickness *r* corresponding to the consumed ceramic (Figure 1a). The position of the initial contact plane, *K* in Figure 1a, between the ceramic and the alloy is marked with alumina platelets. The boundaries between this modified metal/ceramic contact zone and the unaffected ceramic and steel regions are also clearly visible in Figure 1a.

The microstructure of the diffusion zone *d* depends on the composition of the iron alloy. Figures 1b and 1c correspond to diffusion experiments between SN1 ceramic and two steels of different carbon contents, A1 (0.13wt% C) and A3 (1.05wt% C). After etching with an ethanol/1.5% HNO_3 solution (Nital 1,5%), the microstructure of the diffusion zone of the hypo-eutectoid steel A1 shows that there is no pearlite present. This means that the amount of dissolved Si is enough to stabilise the α–Fe solid solution at the reaction temperature over the whole length of the diffusion zone. Pearlitic grains appear

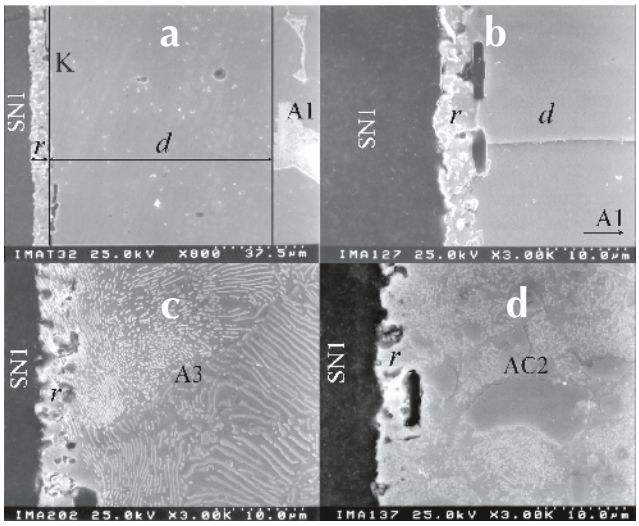

Figure 1 – SEM photomicrographs of diffusion couples of SN1 ceramic after reaction at 1050ºC/80h against (a,b) A1 carbon steel; (c) A3 carbon steel, (d) AC2 chromium alloyed steel. d – diffusion zone in the metal side, r – reaction zone in the ceramic side.

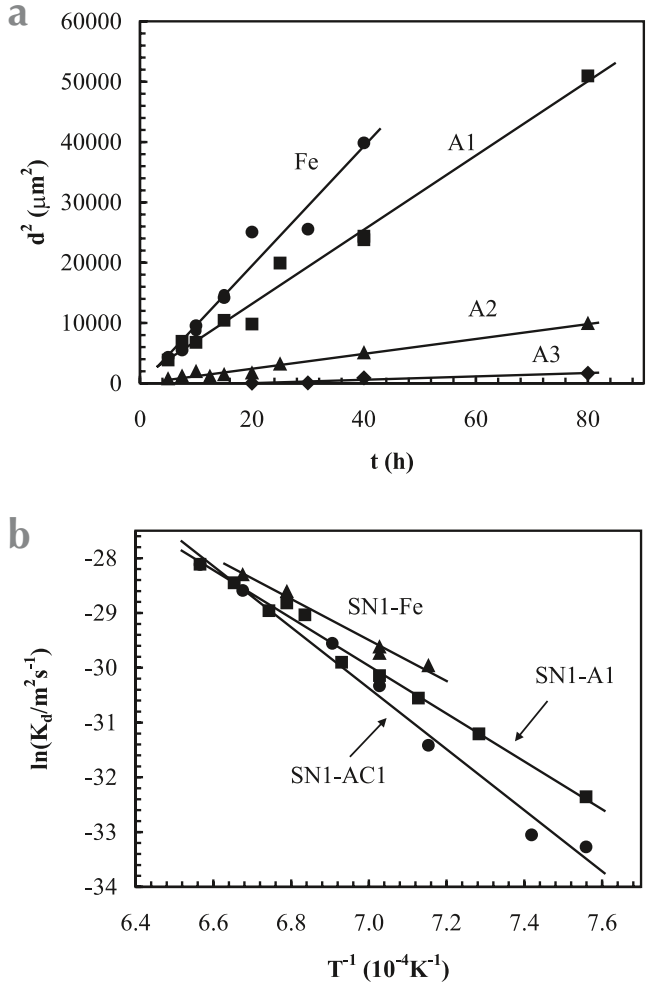

Figure 2 – Effect of steel composition on the diffusion zone formation rate for SN1 ceramic couples with pure iron (Fe) and different steels (A1, A2, A3, AC1). (a) Square of the diffusion zone thickness d at 1150ºC as a function of time; (b) Arrhenius plot of the parabolic diffusion rate constant Kd for the temperature range 1050-1250ºC.

only in the unaffected metal after the diffusion zone (Figure 1a) resulting from the decomposition of the γ-Fe solid solution during cool down to room temperature. On the contrary, the A3 steel keeps its pearlitic structure in the diffusion zone (Figure 1c), because the much higher carbon amount hinders the γ-Fe→α-Fe transformation.

For steel AC2, the very high carbon content also stabilises the γ-Fe phase at the reaction temperature in spite of the presence of the Cr from the steel and Si from the Si_3N_4 ceramic decomposition. Both are α-Fe stabiliser elements. In this particular case, large $(Cr,Fe)_7C_3$ carbide particles are seen in a pearlitic matrix (Figure 1d).

The thickness of the diffusion zone, *d*, or extent of the α-Fe solid solution domain, was measured as a function of time and is reported in Figure 2a for pure iron and the three carbon steels A1, A2 and A3. A parabolic law of time for *d*, $d^2=2K_d.t$ [20], fits the experimental data. Since N diffuses much faster than Si in both iron structures [21,22] the extent of the diffusion zone must be related to the Si concentration profile. The amount of Si dissolved within *d* zone is a measure of the reactivity of the Si_3N_4 ceramic due to the direct relationship between *d* and the thickness of the ceramic reacted zone, *r* [23], significantly decreases with the increasing nominal carbon content of the steel. This is also true for the chromium containing steels that have similar amounts of Cr but quite different C content [23].

The activation energy for the parabolic rate constant K_d increases from 310kJmol^{-1} for pure iron to 360kJmol^{-1} for A1 carbon steel and to about 460kJmol^{-1} for the Cr alloyed steel AC1. These values calculated from the Arrhenius plots in Figure 2b, are comparable to the activation energies measured from similar plots for the reaction zone (320→440kJmol^{-1}) [12]. Stoop and co-author [2] calculated an activation energy of 700kJmol^{-1} in AISI 316 stainless steel/Si_3N_4 couples for the diffusion zone kinetics. This high value was attributed to a mixed control for the reaction, the ceramic decomposition and the diffusion in the metal. The values found in the present work are higher than the activation energy for Si diffusion in α-Fe (240kJmol^{-1}) [22], but closer to 400kJmol^{-1}, a value reported for the Si_3N_4 densification kinetics [24] and for the Si-N bond energy [25]. This is a first indication that the ceramic decomposition, dissolution and diffusion in the intergranular glassy phase are among the slowest steps of the overall reaction kinetics.

The Si concentration profiles measured with the EPMA in the diffusion zone of couples with SN1 against pure iron, A1 and A3 steels, after reaction at 1150ºC for 7.5 hours, are represented in Figure 3a. The integral area under the curves, the amount of dissolved Si, increases in the sequence A3→A1→Fe corresponding to the enhanced reactivity for the alloys with lower carbon content already observed in Figure 2a. The profile shape of Si on the A3 steel differs from those of the low carbon alloy A1 and pure Fe, these two showing a steep decrease on the Si concentration in a plane corresponding to the interface between *d* and the unaffected metal. The last feature was already reported by Heikinheimo [18] and Oliveira et al. [26] in diffusion couples with pure iron and it was attributed to the presence of the α-Fe/γ-Fe phase boundary.

Taking this as a valid assumption we calculated the composition at the α-Fe/γ-Fe solid solution phase boundary for the various steels [23]. The equilibrium thermodynamic calculations at the advancing interfaces on the metallic side of the diffusion couples were done using the ChemSage program

[27] (V. 3.2, GTT Technologies, RWTH) and the SGTE [28] databases for pure substances and solutions. The calculation method used, the assumptions made and the results of thermodynamic modelling are described in another publication [23] where a direct correlation was obtained between the reactivity and the concentration of Si at the α/γ-Fe phase boundary. The calculated Si concentrations necessary to fully stabilise the α-Fe solid solutions are given in Figure 3a for Fe, A1 and A3 steels. These values determine the position of the abrupt decrease in the Si concentration profile and thus the extent of the diffusion zone. This is verified for the low carbon steel A1 and pure iron whereas for the high carbon content steel A3, the Si incorporated was not enough to promote the γ-Fe to α-Fe phase transformation (Figure 3a). In this alloy, Si diffusion occurs only in the close packed fcc structure (γ-Fe) where diffusion coefficients of substitutional elements are the lowest [22].

The Si concentration profiles in the diffusion zone, *d*, of SN1/pure Fe couples reacted at increasing times, are shown in Figure 3b. The value of Si concentration at which the sudden decrease in the profile occurs is the same, irrespectively of the degree of reaction, further confirming the validity of the calculations made.

The effect of the silicon nitride composition on the reaction kinetics was studied in diffusion couples with the steel A1. The compositions of the tested ceramic matrix composites are given in Table I. The set of SEM micrographs presented in Figure 4 compares the microstructures of the diffusion couples after reaction at 1150ºC for 20h. The HfN composite (Figure 4a) is more reactive than the composite with BN (Figure 4b), or TiN (Figure 4c). The more chemically resistant material is the composite SN2-AL with $A1_2O_3$ platelets dispersed in an alumina saturated matrix (Figure 4d). The morphology of the reaction zone results from the decomposition of Si_3N_4 and filling up with Fe the space between the reinforcing particles. The lengths of the diffusion and reaction zones are also interrelated as discussed before for the couples with the un-reinforced ceramic SN1. The larger diffusion zone is observed for the couple with the more reactive ceramic, SN1-HN (Figure 4a) while the smallest value of *d* is measured in the couples with the ceramic composite SN2-AL (Figure 4d).

The extent of the reaction zone, *r*, for these composites in the reaction with carbon steel A1 at 1150ºC is plotted as a function of time in Figure 5. Data for SN1 are also included for comparison. As it happened with the diffusion zone of Figure 2a, a parabolic law fits the experimental data. The compounds TiN, BN, HfN and $A1_2O_3$ should be chemically more stable than Si_3N_4 in the contact with iron at high temperature due to the more negative free energy of formation of these nitrides and of the Al oxide [9]. However, as depicted from Figure 5, only the SN2-AL composite with the $A1_2O_3$ platelets reveals increased resistance to chemical attack by the carbon steel A1, as confirmed by the smaller penetration depth, *r*, into the composite than that into the SN1 matrix. The composites with the compound BN and particularly the one with HfN evidence faster reaction rates than the values obtained for the SN1 matrix or the SN1-TN composite. While TiN particles were inert with respect to the unreinforced matrix during the sintering stage, the BN and HfN reacted to some extent with the intergranular glassy phase [14], increasing the area fraction for Fe diffusion into the ceramic. In the case of the SN2-AL composite, the matrix contains X-SiAlON from the reaction between the added $A1_2O_3$ and Si_3N_4 [16], the stability of the crystalline intergranular phase delaying the corrosion of the ceramic by Fe [29].

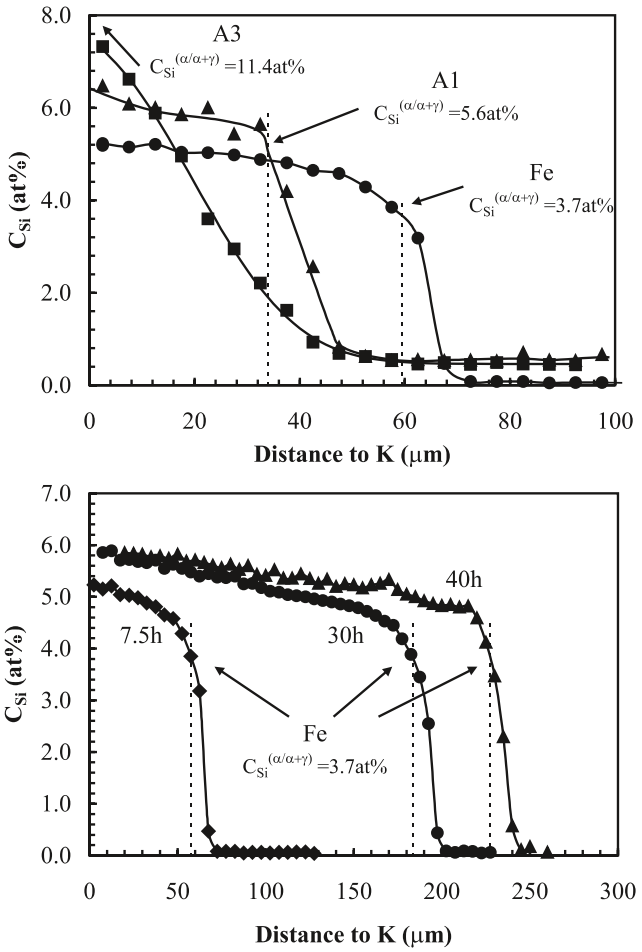

Figure 3 – Si concentration profiles in the diffusion zone of SN1/steel couples tested at 1150ºC. (a) Si concentration in iron, A1 and A3 carbon steels, after reaction for7.5 h; (b) values for pure iron for different reaction times.

Accordingly to these findings we propose that the attack proceeds by Fe penetration through the grain boundary phase into the ceramic followed by the dissolution of the Si_3N_4 grains in the modified glassy phase. The smaller the amount of the intergranular glassy phase the smaller the reaction rates are. The activation energy for the formation of the reaction zone in this composite was calculated as 460kJmol^{-1} [12], a value comparable to the given above for the couples with SN1.

4. CONCLUSIONS

Si_3N_4 decomposes into Si and N that dissolve and diffuse in pure iron, carbon and chromium alloyed steels at temperatures above 1050ºC. Si remains in the alloy diffusion zone adjacent to the ceramic while N escapes to the atmosphere. For low carbon alloys, the dissolved Si is enough to stabilise the α-Fe solid solution at the reaction temperature. In these alloys a sudden decrease in the Si concentration is observed in the plane corresponding to the α-Fe/γ-Fe phase transition. Steels with low carbon content also increase the amount of Si dissolved, the length of the diffusion zone and thus the reactivity of the ceramic.

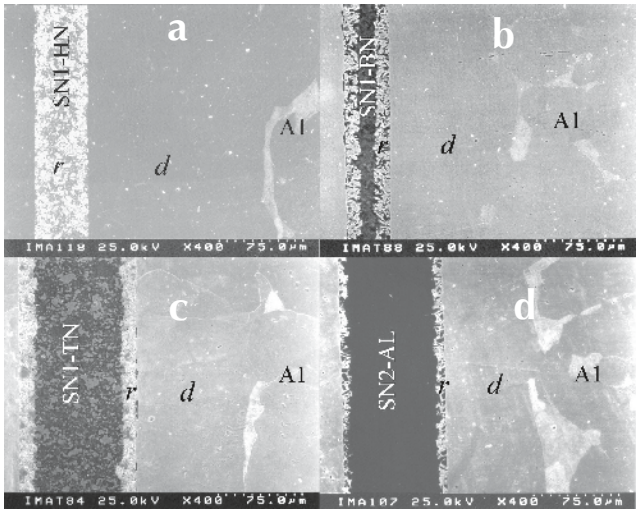

Figure 4 – SEM photomicrographs of diffusion couples of composite ceramics after reaction at 1150ºC/20h with A1 carbon steel. (a) Si_3N_4–HfN composite; (b) Si3N4–BN; (c) Si_3N_4–TiN; (d) Si_3N_4–Al_2O_3. d – diffusion zone in the metal side, r – reaction zone in the ceramic side.

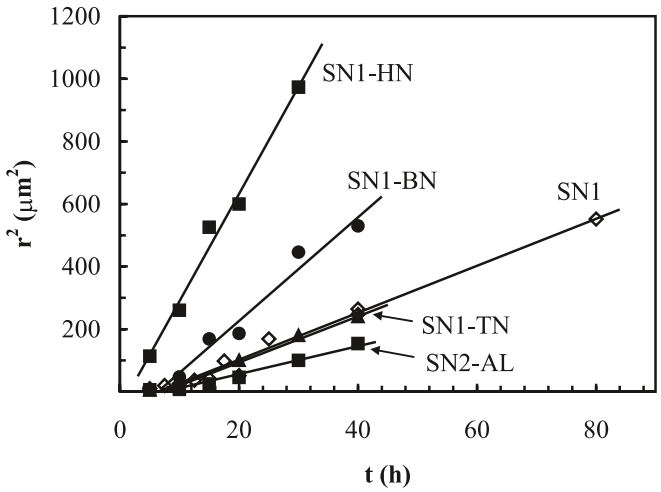

Figure 5 – Effect of ceramic composition on the reaction zone (r) formation rate for diffusion tests with A1 carbon steel at 1150ºC.

The Si_3N_4 composites containing 30vol% of HfN or BN did not show any improvement in the chemical resistance relatively to the unreinforced material, due to unwanted reactivity during the sintering stage between those compounds and the intergranular phase of the matrix. For the TiN-Si_3N_4 composite the reaction rate is the same as for the matrix while for the composite with the $A1_2O_3$ platelets the chemical resistance is enhanced due to the presence of stable crystalline phases as intergranular phases.

Both the diffusion and reaction zones obey a parabolic growth law of time with activation energies for the corresponding rate constants in the range Q=310-460kJmol^{-1}. The activation energies values are closer to values known for the control by diffusion mechanisms of hot-pressing, oxidation or corrosion kinetics in the ceramic than to the values of Si diffusion in the iron alloys.

ACKNOWLEDGMENTS

F. J. Oliveira acknowledges the financial support of the Sub-Programa Ciência e Tecnologia do 2º Quadro Comunitário de Apoio. The financial support under the research contract PRAXIS 3/3.1/MMA/1777/95 is gratefully acknowledged.

REFERENCES

1. K. Saganuma, M. Shimada, T. Okamoto, M. Koizumi. «High Pressure Bonding of Ceramics to Metals». Proc. Brit. Soc. **34** 273-285 (1984)
2. B.T.J. Stoop, G. Den Ouden. «Diffusion Bonding of Silicon Nitride to Austenitic Staninless Steels Without Interlayers». Metal. Trans. A **24** 1835-43 (1993)
3. S.D. Peteves, K. Saganuma. «Solid State Bonding of Si_3N_4 Ceramics with Fe-Cr Alloy Interlayers», pp. 229-238 in *Structural Ceramics Joining II*. Ed. A.J. Moorhead et al. The American Ceramic Society, Ohio (USA) (1992).
4. G. Ceccone, M.G. Nicholas, S.D. Peteves, A.A. Kodentsov, J.K. Kivilahti. «The Brazing of Si_3N_4 with Ni-Cr-Si Alloys». J. Eur. Ceram. Soc. **15** 563-572 (1995).
5. J.A. Yeomans, T.F. Page. «The Chemical Stability of Ceramic Cutting Tool Materials Exposed to Liquid Metals». Wear **131** 163-175 (1989).
6. J. Vleugels, T. Laoui, K. Vercammen, J.P. Celis, O. Van Der Biest. «Chemical Interaction Between a Sialon Cutting Tool and Iron Based Alloys». Mater. Sci. Eng. A **187** [2] 177-182 (1994).
7. R.F. Silva, F.J. Oliveira, J.M. Vieira. «Modelling of Chemical Wear in Ferrous Alloys/Silicon Nitride Contacts During High Speed Cutting». Acta Mater. **7** 2501-2507 (1998).
8. R.F. Silva, J.M. Gomes, A.S. Miranda, J.M. Vieira. «Resistance of Si_3N_4 Ceramic Tools to Thermal and Mechanical Loading in Cutting of Iron Alloys». Wear **148** 69-89 (1991).
9. B.M. Kramer, N.P. Suh. «Tool Wear by Dissolution: A Quantitative Understanding». ASME J. Eng. Ind. **102** [3] 303-309 (1979).
10. J. Vleugels, L. Van Der Perre, O. Van Der Biest. «Influence of Alloying Elements on the Chemical Reactivity Between Si-Al-O-N Ceramics and Iron-Based Alloys». J. Mater. Res. **11** [5] 1265-1276 (1996).
11. S.T. Buljan, S.F. Wayne. «Silicon-Nitride-Based Composite Cutting Tools: Material Design Approach». Adv. Ceram. Mater. **2** [4] 813-816 (1987).
12. F.J. Oliveira, R.F. Silva, J.M. Vieira. «Dissolution of Si_3N_4-$A1_2O_3$ (pl) Composite Tool Materials in Carbon Steels». Key Eng. Mater. **132-136** 2068-2071 (1997).
13. F.J. Oliveira, R.F. Silva, J.M. Vieira. «Interfacial Reaction Kinetics of Silicon Nitride/Iron Alloys Diffusion Couples in the Range 1050ºC-1250ºC», pp.203-209 in *Interfacial Science in Ceramic Joining*. Ed. A. Bellosi et al.. Kluwer Academic Publishers, The Netherlands 1998.
14. F.J. Oliveira, R.F. Silva, J.M. Vieira. «Chemical Reactivity of Silicon Nitride Composites with Oxide, Nitride, and Carbide Dispersoids Against Carbon Steel». J. Mater. Synth. Process. **6** [4] 287-290 (1998).
15. G. R. Anstis, P. Chantikul, B. R. Lawn, D. B .Marshall. «A Critical Evaluation of Indentation Techniques for Measuring Fracture Toughness». J. Am. Ceram. Soc. **64** [9] 533-538 (1981).
16. F.J. Oliveira, R.F. Silva, J.M. Vieira. «Densification and Microstructural Evolution in a Reactive Silicon Nitride/Alumina Platelet System». Key Eng. Mater. **127-131** 377-384 (1997).
17. K. Frisk. «A Thermodynamic Evaluation of the Cr-Fe-N System». Met. Trans. A **21** 2477-2488 (1990).
18. E. Heikinheimo, I. Isomaki, A. Kodentsov, F. J. van Loo. «Chemical Interaction Between Fe and Silicon Nitride Ceramic». J. Eur. Ceram. Soc. **17** 25-32 (1997).
19. T. Shimoo, T. Yamasaki, K. Okamura. «Interaction of Si_3N_4 with Carbonyl Iron under Nitrogen or Argon Atmosphere». J. Ceram. Soc. Japan **105** [9] 734-739 (1997).
20. F.J.J. Van Loo. «Multiphase Diffusion in Binary and Ternary Solid-State Systems». Prog. Sol. State Chem. **20** 47-99 (1990).
21. R. W. Honeycomb. «Steels – Microstructure and Properties», pp.19. Edward Arnold Publishers Ltd, London 1982.
22. H. Oikawa. «Lattice Diffusion of Substitutional Elements in Iron and Iron-Base Solid Solutions. A Critical Review». Technol. Rep. Tohoku Univ. **48** [1] 7-77 (1983).
23. F.J. Oliveira, R. F. Silva, J.M. Vieira. "Thermochemistry of Contacts between Silicon Nitride Ceramics and Steels", Acta Mater. (Accepted for publication).
24. R.F. Silva, A.P. Moreira, J.M. Gomes, A.S. Miranda, J.M. Vieira. «The Role of Nitrogen in the Intergranular Glass Phase of Si_3N_4 on High Temperature Applications and Wear». Mater. Sci. Eng. A **168** 55-59 (1993).
25. A.E. Pasto. «Causes and Effects of Fe-Bearing Inclusions in Sintered Si_3N_4» J. Am. Ceram. Soc. **67** [9] C178-C180 (1984).
26. F.J. Oliveira, R.F. Silva, J.M. Vieira. «The Sequential Testing in the Study of Si_3N_4/Fe Diffusion Couples» pp.947-954 in *Ceramics: Getting into the 2000's-Part C*, 9th Cimtec-World Ceramics Congress, Ed. P. Vincenzini. Techna Srl, Faenza (Italy) 1999.
27. G. Eriksson, K. Hack. «ChemSage – a Computer Program for The Calculation of Complex Chemical Equilibria». Met. Trans. B **21** 1013-1023 (1990).
28. National Physical Laboratory, Internet Site UK, http://www.npl.co.uk/ npl/cmmt/mtdata/sgte.htm.
29. Y. Zhou, J. Vleugels, T. Laoui, P. Ratchev, O. van der Biest. «Preparation and Properties of X-SiAlON». J. Mater. Sci. **30** 4584-4590 (1995).

Recibido: 19.10.99
Aceptado: 29.02.00